Psychiatry Research: Neuroimaging 321 (2022) 111444

Contents lists available at ScienceDirect

Psychiatry Research: Neuroimaging

journal homepage: www.elsevier.com/locate/psychresns

Altered Resting State Functional Connectivity and Its Correlation with Cognitive Functions at Ultra High Risk for Psychosis

Oznur Bulbul [a,*], Elif Kurt [b,c], Cigdem Ulasoglu-Yildiz [b,d], Tamer Demiralp [b,e], Alp Ucok [f]

[a] Department of Psychiatry, Erenkoy Training and Research Hospital for Psychiatric and Neurological Diseases, Istanbul, Turkey
[b] Hulusi Behçet Life Sciences Research Laboratory, Istanbul University, Çapa, Istanbul 34093, Turkey
[c] Department of Neuroscience, Aziz Sancar Institute of Experimental Medicine, Istanbul University, Çapa, Istanbul 34093, Turkey
[d] Department of Psychology, Faculty of Humanities and Social Sciences, Istinye University, Istanbul, Turkey
[e] Department of Physiology, Istanbul Faculty of Medicine, Istanbul University, Çapa, Istanbul 34093, Turkey
[f] Department of Psychiatry, Faculty of Medicine, Istanbul University, Istanbul, Turkey

ARTICLE INFO

Key words:
Ultra high risk psychosis (UHR)
Neuroimaging
Functional magnetic resonance imaging (fMRI)
Resting state
Cognitive function

ABSTRACT

The aim of this study is to identify robust resting state-functional connectivity (rs-FC) alterations and their correlations with the neuropsychological characteristics of Ultra-High Risk (UHR) for psychosis subjects compared to healthy controls (HCs). Twenty individuals with UHR and sixteen HCs underwent resting-state functional magnetic resonance imaging (rs-fMRI) and a cognitive battery evaluating attention, episodic memory and executive functions. Compared to HCs, UHR individuals showed working memory and set-shifting impairments. In functional connectivity (FC) analyses, the Default Mode Network (DMN) of the UHR subjects displayed increased FC with the visual areas and decreased FC with the Dorsal Attention Network (DAN). Additionally, the salience network (SN) of the UHR subjects displayed increased connectivity with wide posterior cortical areas in the temporal, parietal and occipital lobes, corresponding to posterior nodes of the SN itself, the Somato-Motor Network (SMN) and the DAN. The SN connectivity with the left SMN and DAN was positively correlated with the Trail Making Test - B scores of the UHR subjects. These findings show that the SN and DMN, which mostly show abnormal connectivity patterns in psychosis, are also affected in UHR subjects, while the SN plays a more central role with its hyperconnectivity to the DAN and SMN.

1. Introduction

A prodromal period which is characterized by subthreshold psychotic symptoms and decreased social and occupational functioning usually precedes the onset of psychotic disorders. Ultra-high risk (UHR) criteria (Yung et al., 2005) are commonly used to identify individuals at a high risk for the development of psychosis. The rate of conversion to psychosis at the end of 3 years of UHR individuals is 36% (Fusar-Poli et al., 2012a). Cognitive dysfunction is a major deficiency in schizophrenia, and cognitive performance of the UHR individuals for psychosis are reported as worse than healthy individuals but less severe than first episode of schizophrenia (Ucok et al., 2013; Chu et al., 2018; Hou et al., 2016). While the neuropsychological evaluation of the cognitive functions provides a predictive value for conversion to psychosis in UHR individuals (Kim et al., 2011), still other markers are needed to predict precisely which individuals in the ultra-high-risk group will develop psychosis, in order to selectively apply preventive clinical interventions only to this subgroup (Fusar-Poly et al, 2012).

Neuroimaging techniques have significantly improved our understanding of the pathophysiology of UHR (Gifford et al., 2017), and have provided results about the presence of structural, neurochemical and functional abnormalities in UHR subjects similar to those in schizophrenia patients (Morey et al., 2005; Borgwardt et al., 2007; Howes et al., 2009; Allen et al., 2016; Bloomfield et al., 2016; Hubl et al., 2018). Among the neuroimaging modalities, the functional measurements are considered more sensitive to early changes in the progression of neuropsychiatric disorders, before manifest structural, perfusion or neurochemical differences can be detected later in the course of the disease. Therefore, fMRI and specifically rs-fMRI data recorded without a specific task in standard clinical imaging settings presents the feasibility and a higher potential to provide early biomarkers for predicting the conversion to psychosis (Collin et al., 2020).

* Corresponding author.
E-mail address: oznurtabak@gmail.com (O. Bulbul).

https://doi.org/10.1016/j.pscychresns.2022.111444
Received 10 March 2021; Received in revised form 6 January 2022; Accepted 17 January 2022
Available online 21 January 2022
0925-4927/© 2022 Elsevier B.V. All rights reserved.

Rs-fMRI mainly evaluated by computing the temporal relationship between fMRI signals of distinct brain regions at various spatial scales or by decomposing the whole brain fMRI data into a set of temporally coherent and spatially independent components (IC), may provide information about various aspects of the resting-state functional connectivity (rs-FC) in the brain according to the selection of the computation method and/or the seed regions. A wide spectrum of the rs-FC analyses based on one of these two main techniques provide spatial maps of a set of large-scale intrinsic connectivity networks (ICN), which reflect the integration of the ongoing neural activities among distinct brain regions during rest. Among the ICNs, the task-negative Default Mode (DMN) and task-positive Salience (SN), Executive Control (ECN) and Dorsal Attention (DAN) networks are strongly associated with cognitive and affective functions.

The triple network model of aberrant saliency mapping and cognitive dysfunction proposed by Menon (2011) for evaluating the network dynamics of the psychopathologies focuses on the first three of the above networks and the aberrant coupling among them, and is widely studied in the psychosis spectrum disorders (O'Neil et al., 2019). On the other side, other studies focused on the rs-FC of circuitries overarching these network patterns, such as the thalamo-cortical circuitry (Anticevic et al., 2015), or representing specific sub-components of these networks such as the amygdalo-prefrontal circuitry (Ho et al., 2019). Such rs-FC analyses generally revealed significant differences in the UHR subjects compared with healthy controls (Anteraper et al., 2020; Anticevic et al., 2015; Cooper et al., 2014; Dandash et al., 2014; Wang et al., 2016; Wotruba et al., 2014; Zhu et al., 2019), which were similar to those found in patients with schizophrenia (Brandl et al., 2019; O'Neill et al., 2019). However, the variety of the analytical approaches have also resulted in divergent and partly contradictory results. This complicates the integration and comparison of the reported findings in terms of their sensitivity to the characterization of the early disease processes, which is important for narrowing the search area for a potential functional neuroimaging biomarker for conversion from UHR to psychosis.

The aim of the present study is to explore the whole brain connectivity patterns of the seed regions that provided consistent results in the psychosis literature by a seed-to-voxel analysis in order to compare their sensitivity to early disease processes and to cognitive impairment. As seed-to-voxel FC analyses allow the evaluation of both circuit- and network-level differences as well as the intra- and inter-network changes flexibly at the voxel level, such exploration may provide important insight about the potential neuroimaging biomarkers for progression to psychosis. Since previous studies and meta-analyses on UHR subjects and schizophrenic patients indicated consistent and central changes in the DMN, SN and thalamo-cortical and amygdalo-prefrontal circuitry (Anticevic et al., 2015; Ho et al., 2019; O'Neill et al., 2019), we chose the widely investigated and validated core nodes of the DMN and SN networks, thalamus and amygdala as seed regions. We hypothesize that a subset of these investigated rs-FC patterns will be proven to be more sensitive to early neurophysiological changes in UHR and will be correlated with cognitive functions. As a result, we expect that our result will shed light on potential rs-fMRI markers that can be investigated in longitudinal studies on larger samples.

2. Methods

2.1. Participants

This study was conducted in the Psychotic Disorders Research Program, Istanbul Faculty of Medicine. The local ethics panel of the Istanbul University, Istanbul Faculty of Medicine approved the study. Twenty individuals with UHR and sixteen healthy comparison subjects were recruited. The Ultra-high-risk status was defined using the Comprehensive Assessment of At-Risk Mental States (CAARMS) (Yung et al., 2005; Yokuşoğlu et al., 2020). The individuals were defined as at UHR if they met the criteria of at least one of the following conditions: (1) Brief limited intermittent psychotic symptoms (BLIPS); frank psychotic symptoms last less than one week and resolve without treatment, (2) Attenuated psychotic symptoms, (3) Vulnerability group; a recent decline in function, together with either the presence of schizotypal personality disorder or a family history of psychosis in a first degree relative. Individuals were evaluated by a senior psychiatrist (A.U). The subjects recruited were antipsychotic naive. Healthy comparison subjects ($N = 16$) were recruited from the local community. All participants completed an informed consent form for the study. Exclusion criteria were as follows: Unwillingness to participate, illiteracy, mental retardation, prior antipsychotic treatment, severe medical condition, neurological illness, considerable head injury, prior history of psychosis that lasted more than a week, and present alcohol and substance abuse, contraindication to scanning.

2.2. Procedure and instruments

Patients were administered the Brief Psychiatric Rating Scale-expanded (BPRS) (Lukoff et al., 1986), the Scale for the Assessment of Negative Symptoms (SANS) (Andreasen, 1983), the Scale for the Assessment of Positive Symptoms (SAPS) (Andreasen, 1984), the Calgary Depression Scale for Schizophrenia (CDSS) (Addington et al., 1992). In order to evaluate executive function and attention, Wisconsin Card Sorting Test (WCST) (Heaton et al., 1993), Trail Making Test (TMT) (Reitan., 1955), Digit Span Test and Digit Symbol Substitution Test of the Wechsler Adult Intelligence Scale - Revised (WAIS-R) sub-tests (Wechsler, 1981), Stroop Test (Golden, 1978) (), and Verbal Fluency Test were performed. Rey Auditory Verbal Learning Test (RAVLT) (Rey, 1964) was used for testing the episodic memory.

2.3. MRI data acquisition

MRI data were acquired at Istanbul University Hulusi Behcet Life Sciences Research Laboratory with a 3 T scanner (Philips Achieva, Best, The Netherlands) with 32-channel head coil. High resolution T1-weighted structural 3D images were acquired with the following parameters: repetition time/echo time (TR/TE): 7.7/3.8 ms, field of view (FOV): 250 × 250 mm, 160 axial slices and 1 mm^3 voxel size. Resting-state fMRI data were obtained using an echo planar imaging (EPI) sequence with the following parameters: TR: 2000 ms, TE: 30 ms, flip angle: 90°, FOV: 224 × 240 mm, acquisition matrix size: 112 × 117 and voxel size: 2 × 2 × 4 mm^3 in-plane resolution. Following 10 dummy volumes, 214 vol each containing 36 axial slices covering the whole brain, were obtained with a total scan time of 448 s. All participants were instructed to remain awake and lie in the most relaxed position with closed eyes.

2.4. MRI data preprocessing

The data were preprocessed using SPM 12 (Statistical Parametric Mapping version 12; http://www.fil.ion.ucl.ac.uk/spm/) and CONN functional connectivity toolbox version 20.b (https://www.nitrc.org/projects/conn) (Whitfield-Gabrieli and Nieto-Castanon, 2012). First, the functional images were realigned to the first image in order to correct for head motion. Then the Artifact Detection Tools (ART) toolbox (https://www.nitrc.org/projects/artifact_detect; implemented in CONN's preprocessing pipeline) was used for the identification of outlier scans in terms of excessive subject motion and signal intensity spikes. The global-signal (GS) z-value threshold for signal intensity outliers was set at 5 standard deviations (SD) greater than or less than the mean intensity of the entire session, and the threshold for the frame-wise displacement (FD) (Power et al., 2012) was set as $\geq$ 0.9 mm difference in composite motion of an image from the previous scan. There were no participants with outliers more than 20% (>43) of the total number of functional volumes (214), so no participants were excluded from further analyses. Additionally, to control the head motion difference between the two

groups, mean FD, number of outlier scans, mean GS change and mean motion calculated for each subject and were compared between the two groups using Mann–Whitney U-tests.

Afterwards, functional and structural data were coregistered. Then, the structural images were segmented into white matter (WM), gray matter, and cerebrospinal fluid (CSF), and normalized to the Montreal Neurological Institute (MNI) standard space. Using the resulting transformation matrix, the functional data were also spatially normalized and resampled to 2 mm^3 isotropic voxels. Finally, the functional data were smoothed by spatial convolution with an isotropic Gaussian kernel (full width half maximum = 8 mm).

The default denoising procedure as defined in the CONN toolbox was applied on the functional data to remove the effects of potential noise sources related with the movement and physiological effects. With this procedure, potential noise components derived from WM and CSF signals were estimated and included as confounds in the denoising step. Six subject motion parameters (three translation and three rotation values) obtained in the realignment step, their first order derivatives and the outlier scans defined with ART procedure were also included as confounds. Finally, effect of the scanning session was included into confounding effects in order to decrease the influence of slow, linear trends in BOLD signal. Finally, a temporal bandpass filter of 0.01−0.1 Hz was applied to the functional images in order to reduce the effects from noise sources at lower and higher frequency ranges.

2.5. Functional connectivity analyses

Seed-to-voxel functional connectivity (FC) analysis was performed using the CONN toolbox. A total of 15 seeds selected based on the current rs-FC literature on the schizophrenia were used for the analysis. Default mode network (DMN) and salience network (SN) seeds were based on the network atlas implemented in the CONN toolbox, and right and left thalami and amygdalae were based on the FSL Harvard-Oxford Atlas. The seeds for the DMN were medial prefrontal cortex (MPFC), right and left lateral parietal (LP) cortices and posterior cingulate cortex (PCC). Those for the SN were anterior cingulate cortex (ACC), right and left anterior insulae (AI), right and left rostral prefrontal cortices (RPFC) and right and left supramarginal gyri (SMG). The seed regions are shown in Fig. 1.

Bivariate correlation coefficients were calculated for each subject between the average time-course for each seed region with the time courses of all other voxels in the brain. The Fisher transformation was used to convert the correlation coefficients into Z-scores which were then used in second-level analyses. Two sample t-tests were performed to examine differences in resting-state functional connectivity (rs-FC) between the UHR and HC groups. The voxel-based functional connectivity results were thresholded using an initial cluster-forming threshold set at $p < 0.001$ (uncorrected) followed by cluster-level thresholding at FWE-corrected $p < 0.05$. These results were further Bonferroni corrected for multiple comparisons by adjusting the alpha level for the number of seeds (15) reaching a significance threshold at $p_{\text{FWE-corr}} < 0.003$ (0.05/15).

2.6. Statistical analyses

IBM SPSS version 21 was used for the statistical analyses on the demographical, clinical and neuropsychological variables and correlation analyses. Chi-square test was used for comparing categorical variables and Mann–Whitney U test was used for variables not normally distributed.

2.6.1. Correlation analysis

To investigate the relation between the clinical and cognitive measures and the significant FC changes between the UHR and HC groups, Spearman's correlation coefficients were calculated. Accordingly, the significant voxel clusters obtained in the between-group comparisons were defined as regions of interests (ROIs), and the averaged Fisher's z-transformed rs-FC values of these ROIs were extracted for each subject by using the ROI extraction tool (REX) of the CONN toolbox.

The correlations between the averaged rs-FCs of the ROIs and (i) the clinical scores (BPRS, SANS, SAPS and CDSS), and (ii) cognitive scores of the UHR subjects and (iii) the cognitive scores of the HC subjects were analysed. The following neuropsychological test scores were included in the correlation analyses: Number of completed category and percentage of perseverative errors of WCST, time to completion TMT-A and TMT-B, forward and backward scores of Digit Span test, number of the correct matches of Digit Symbol test, interference score of Stroop test, total score of verbal fluency test, learning and delayed recall of RAVLT. Statistical test results were Bonferroni corrected for the number of ROIs by either the number of clinical scores (4) or the number of multiple comparisons for the number of clinical (4) or neuropsychological (11) scores, respectively.

3. Results

3.1. Demographics and clinical characteristics

The clinical and socio-demographic characteristics of the UHR and HCs groups are presented in Table 1. There were no significant differences between UHR and HCs groups in terms of age, years of education

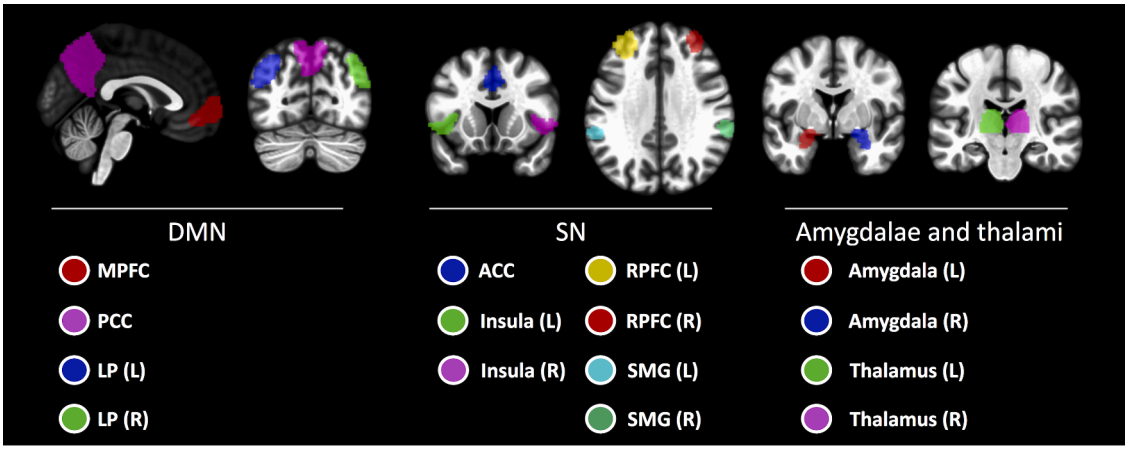


Fig. 1. Cortical regions of interest that were chosen as seeds to probe the DMN and SN in addition to left and right amygdalae and thalami seeds. DMN: default mode network, MPFC: medial prefrontal cortex, LP: lateral parietal, PCC: posterior cingulate cortex, SN: salience network, ACC: anterior cingulate cortex, RPFC: rostral prefrontal cortex, SMG: supramarginal gyrus, L: left, R: right.

Table 1
Demographical and clinical characteristics of the UHR and HCs groups included in rs-FC analysis.

	UHR (n=20) Mean (SD)	HCs (n=16) Mean (SD)	*p*
Age (years)	20.2 (5.27)	18.88 (4.26)	0.49
Gender (Female/Male)	4/16	4/12	0.72
Education (years)	10.8 (3.02)	10.69 (% 2.24)	0.974
Schizophrenia in first degree relatives (%)	%20		
BPRS total score	50.63 (8.12)		
SAPS total score	18.68 (11.13)		
SANS total score	40.63 (18.86)		
CDSS score	6.94 (5.27)		

SD: Standard deviation, BPRS: Brief Psychiatric Rating Scale, SAPS: Scale for Assesment Positive Symptoms, SANS: Scale for Assesment Negative Symptoms, CDSS: Calgary Depression Scale for Schizophrenia

and sex (all p values > 0.05).

No significant differences were found between the groups in terms of episodic memory (RAVLT), as well as attention (digit-span forward) scores as detailed in Table 2. UHR patients did not show any executive function deficit in WCST, Stroop Test and Verbal Fluency Test (all p values > 0.0045). However, they displayed impaired performance on TMT-B ($p = 0.0013$) and Digit Symbol Substitution Test of WAIS-R ($p = 0.0005$), both of which evaluated working memory and set-shifting abilities (Table 2).

3.2. Resting state functional connectivity findings

There were no significant differences between the UHR group and HCs in mean FD ($U = 103$, $p = 0.070$), number of outlier scans ($U = 118.5$, $p = 0.115$), mean GS change ($U = 136$, $p = 0.445$) and mean motion ($U = 107$, $p = 0.092$) pointing to the comparable signal quality in both groups.

Seed-to-voxel functional connectivity analyses conducted on the resting-state fMRI data with 15 seeds revealed significant differences between the two groups for 4 of the seeds including two DMN seeds (MPFC and left LP cortex seeds) and two SN seeds (left and right RPFC) (Table 3).

3.2.1. DMN-related results

MPFC seed of the DMN revealed a significant hyperconnectivity in the UHR compared to the HC group with a cluster corresponding to the left calcarine cortex, lingual gyrus and inferior occipital gyrus (IOG) ($p_{\text{FWE-corr}} = 0.000007$) (Fig. 2).

Table 2
Neuropsychological characteristics of the UHR and HCs groups.

	UHRMean (SD)	HCsMean (SD)	*U*	*p*[a]
WCST category	5.95 (2.72)	7.06 (2.17)	116	0.243
WCST perseverative errors (%)	14.13 (8.91)	13.56 (9.34)	116	0.892
TMT-A (sec)	38.56 (15.23)	28.56 (9.07)	83..5	0.036
TMT-B (sec)	112.05 (54.69)	62.62 (11.56)	58	**0.0013**
Digit span forward	6.5 (2.53)	7.87 (1.96)	75.5	0.047
Digit span backward	5.5 (2.06)	7.19 (2.34)	72	0.035
Digit symbol matches (#)	56.69 (16.01)	78.87 (10.96)	28.5	**0.0005**
Stroop interference (sec)	41.89 (15.17)	36.6 (14)	107.5	0.325
Verbal fluency (total)	38.67 (15.13)	42.62 (7.77)	106.5	0.599
RAVLT learning (trials 1–5)	55.17 (8.97)	59.69 (5.31)	96.5	0.102
RAVLT delayed recall	12.39(2.87)	13.5 (1.63)	114.5	0.313

SD: Standard deviation, RAVLT: Rey Auditory Verbal Learning Test, TMT: Trail Making Test, WCST: Wisconsin Card Sorting Test.

[a] Bonferroni corrected alpha level set at $p < 0.0045$ (0.05/11, according to number of neuropsychological test scores). Significant results are shown in bold.

The left LP cortex seed of the DMN also revealed a significant hyperconnectivity with a cluster corresponding to the left calcarine cortex in the UHR group compared to the HCs ($p_{\text{FWE-corr}} = 0.0003$) (Fig. 3).

Additionally, left LP cortex seed of the DMN revealed a significant hypoconnectivity with a cluster corresponding to the left superior parietal lobule (SPL) and inferior parietal lobule (IPL) in the UHR group ($p_{\text{FWE-corr}} = 0.002996$) (Fig. 4).

3.2.2. SN-related results

Left RPFC seed of the SN revealed a significant hyperconnectivity with a cluster corresponding to the left postCG and SPL in the UHR group compared to the HCs ($p_{\text{FWE-corr}} = 0.000014$) (Fig. 5).

Lastly, right RPFC seed of the SN revealed significant hyperconnectivities with 3 different clusters in the UHR group compared to the HCs. The significant clusters correspond (i) to the right superior temporal gyrus (STG) and middle temporal gyrus (MTG), (ii) to the right SPL and superior occipital gyrus (SOG) and (iii) to the left postCG and SPL ($p_{\text{FWE-corr}} = 0.000011$; $p_{\text{FWE-corr}} = 0.000028$; $p_{\text{FWE-corr}} = 0.0008$, respectively) (Fig. 6).

3.3. Correlations with functional connectivity changes

The 7 significant clusters obtained in the between-group rs-FC comparisons were defined as ROIs for the correlation analyses. The averaged rs-FC values of the 7 ROIs did not reveal significant correlations with any of the 4 clinical scores of the UHR patients after Bonferroni correction with alpha level set at $p < 0.0018$ (0.05/28; 4 clinical scores x 7 ROIs).

Among the correlations of the 7 ROIs with the 11 neuropsychological test scores, after Bonferroni correction at adjusted alpha level $p < 0.0006$ (0.05/77), only the SN (left RPFC) hyperconnectivity to the left postcentral gyrus and superior parietal lobule was positively correlated with the TMT-B scores of the UHR group ($r = 0.737$, $p = 0.0003$) (Fig. 7). HC group did not demonstrate any significant correlation between the neuropsychological test scores and mean rs-FC of the ROIs.

4. Discussion

In the present study, the rs-FC of the thalamus and amygdala did not reveal any significant differences between the UHR and control groups, although significant results were reported in previous studies (Anticevic et al., 2015). However, significant rs-FC differences were obtained in seed-to-voxel FC estimates of both the DMN and SN seed regions. When the clusters that significantly differed between the UHR and HC groups were compared with a widely referred parcellation scheme of the cerebral cortex into 7 large-scale networks (Schaefer et al., 2018), our results indicate that the SN displayed differences in its intra-network connectivity, and both DMN and SN displayed differences in their connections with specific areas of the sensory networks and the dorsal attention network (DAN).

Specifically, the MPFC and the left LP cortex seeds of the DMN displayed significant FC increases with the occipital visual regions including the primary visual cortex, while a significant FC decrease was obtained between the DMN-left LP seed and the left superior and inferior parietal lobules, which mostly overlap with the DAN regions. On the other hand, the right RPFC seed of the SN showed increased FC with temporal, parietal and occipital cortices covering the areas that correspond to the right posterior component of the SN and bilateral SMN and DAN areas. Similarly, the left RPFC seed of the SN was more strongly connected in UHR subjects with the left parietal cortex areas, where a part of the cluster in the post-central gyrus corresponded to SMN and other part in the superior parietal lobule to regions of the DAN. In short, the SN connectivity changes point to an increased intra-network connectivity of the SN, and to increased inter-network connectivity of the SN with both the SMN and DAN.

Table 3
Seed-to-voxel rs-FC results at height threshold $p < 0.001$ uncorrected combined with a cluster level FWE-corrected threshold $p < 0.003$ (0.05/15 seed regions) for the UHR vs HC group comparisons.

Seed Region	Regions showing altered connectivity	Contrast	Peak Coordinate (x y z)	Cluster Voxel Size	T_{max}	$p_{FWE\text{-}corr}$
DMN – MPFC	L calcarine cortex, lingual gyrus and IOG	UHR > HC	-32 -72 -6	848	5.85	0.000007
DMN – LP (L)	L calcarine cortex	UHR > HC	0 -96 -2	548	5.56	0.0003
	L SPL and IPL	UHR < HC	-32 -64 62	388	5.28	0.002996
SN – RPFC (L)	L postCG and SPL	UHR > HC	-22 -44 56	829	5.7	0.000014
SN – RPFC (R)	R STG and MTG	UHR > HC	56 -46 6	832	4.81	0.000011
	R SPL and SOG		10 -48 56	749	5.26	0.000028
	L postCG and SPL		-14 -38 58	477	5.46	0.0008

DMN: default mode network, IOG: inferior occipital gyrus, IPL: inferior parietal lobule, LP: lateral parietal, MPFC: medial prefrontal cortex, MTG: middle temporal gyrus, postCG: postcentral gyrus, RPFC: rostral prefrontal cortex, SN: salience network, SOG: superior occipital gyrus, SPL: superior parietal lobule, STG: superior temporal gyrus, L: left, R: right, x: sagittal, y: coronal, z: axial coordinates.

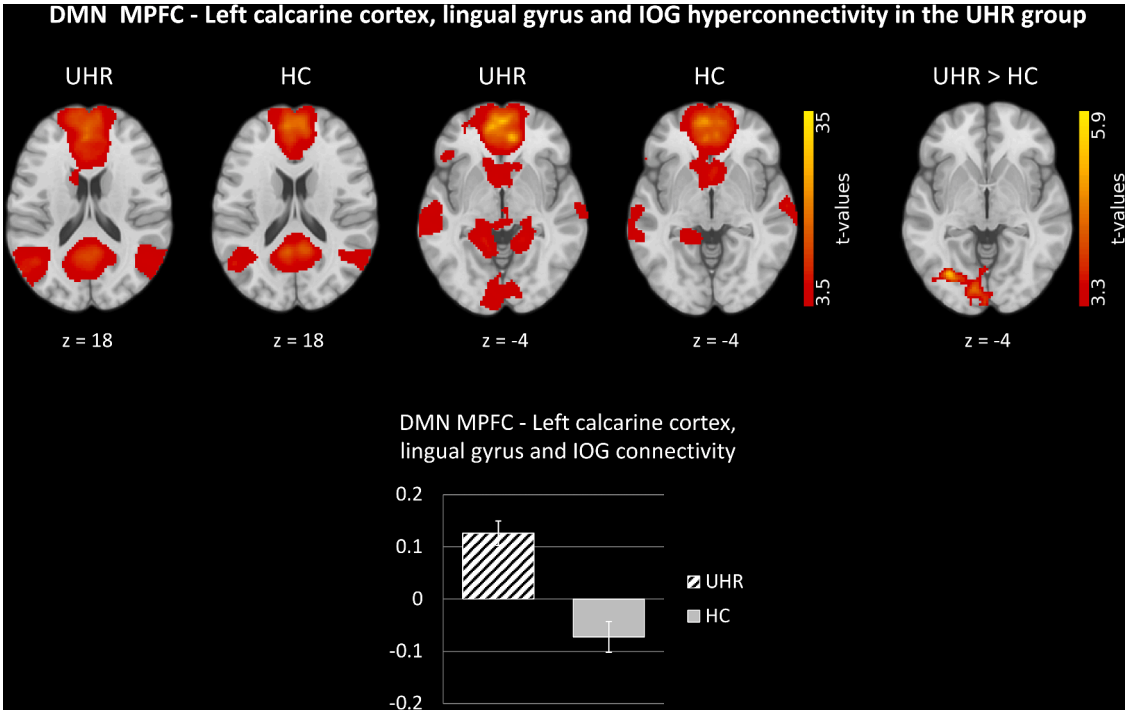


Fig. 2. Hyperconnectivity of the medial prefrontal cortex (MPFC) seed of the default mode network (DMN). The DMN connectivity maps using the MPFC as a seed region for both UHR and HC groups were shown. The UHR group ($N = 20$) displayed increased functional connectivity with the left calcarine cortex, lingual gyrus and inferior occipital gyrus (IOG) compared to HCs (N = 16) (cluster size: 848 voxels; $p_{FWE\text{-}corr} < 0.001$). The result is superimposed on the MNI-152-T1 standard image. Color map represents *t*-values. Bar graph indicates group-averaged z-values extracted from the significant cluster while error bars represent standard errors.

From neuropsychological point of view, UHR subjects showed impairment in speed, working memory and executive functions such as cognitive flexibility and set-shifting abilities. While the mean FC values of the DMN and SN associated significant clusters did not reveal significant correlations with the clinical scores of the UHR subjects, the set-shifting impairment observed in TMT-B was positively correlated with the increased connectivity of the left SN-RPFC seed with the left SMN and DAN areas.

4.1. DMN results

DMN, generally involved in psychoses, plays role in internally-directed thought processes, autobiographical memory, and thinking of others' perspectives (Buckner et al., 2008). Studies have reported mixed findings regarding the resting state connectivity of the DMN in schizophrenia and individuals at high risk for psychosis. While some studies showed hyper-connectivity within the DMN in UHR (Shim et al., 2010; Clark et al., 2018) and increased low frequency fluctuation amplitudes in first-episode schizophrenia subjects (Guo et al., 2017), other studies on early psychosis showed hypo-connectivity within the DMN (Gong et al., 2020; Sharma et al., 2018; Zhao et al., 2018). Wang and co-workers (2018) reported both hypo- and hyper-connected areas within the DMN, and a number of other studies reported aberrant connectivity of the DMN to various cortical and subcortical regions (Anteraper et al., 2020; Pelletier-Baldelli et al., 2018), which include also aberrant coupling of the DMN with the SN and ECN (Menon, 2011; Lee t al., 2018; O'Neil et al., 2019), the components of the proposed triple-network model of psychopathology. In the present study, UHR subjects produced similar intrinsic DMN connectivity patterns as the healthy controls with neither significant intra-network FC differences nor differences in the inter-network coupling with SN or CEN regions. A similar result about the absence of a DMN intrinsic connectivity difference in schizophrenia is also reported before by Kraguljac and co-workers (Kraguljac et al., 2015). However, our results show that the DMN displayed an increased connectivity with the visual network (VN) areas including the calcarine, lingual and inferior occipital cortices and a reduced connectivity with a left DAN area that includes the left superior and inferior parietal lobules.

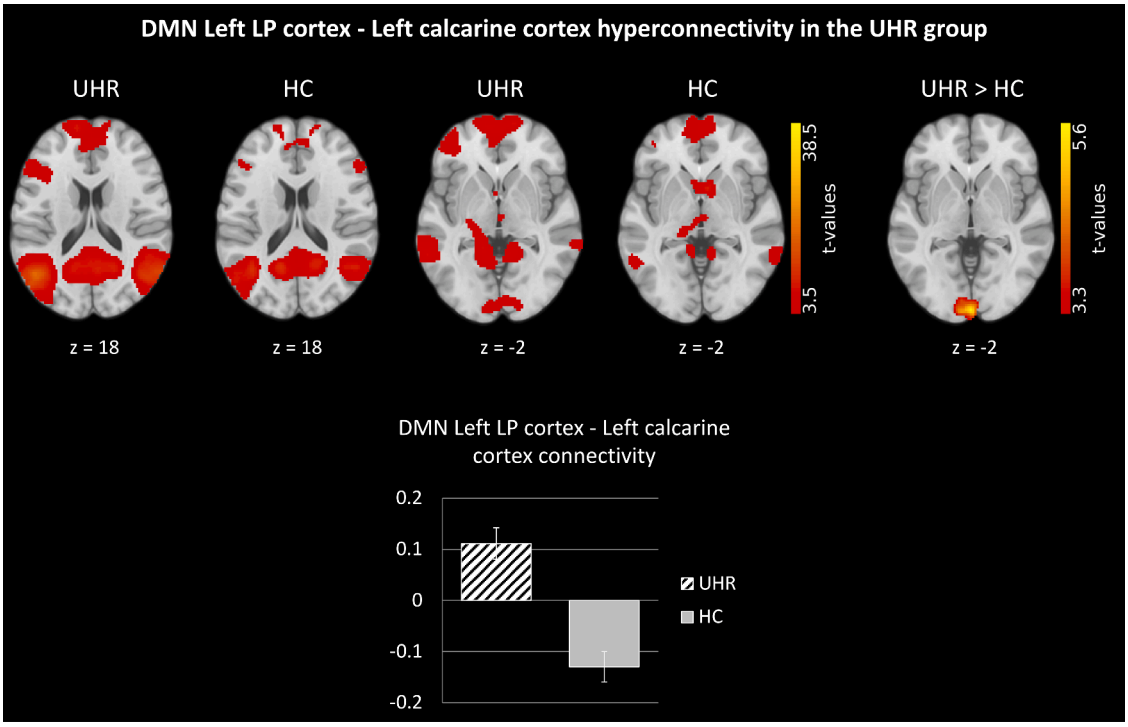


Fig. 3. Hyperconnectivity of the left lateral parietal (LP) cortex seed of the default mode network (DMN). The DMN connectivity maps using the left LP as seed region for both UHR and HC groups were shown. The UHR group ($N = 20$) displayed increased functional connectivity with the left calcarine cortex compared to HCs ($N = 16$) (cluster size: 548 voxels; $p_{FWE\text{-}corr} < 0.001$). The result is superimposed on the MNI-152-T1 standard image. Color map represents *t*-values. Bar graph indicates group-averaged z-values extracted from the significant cluster, while error bars represent standard errors.

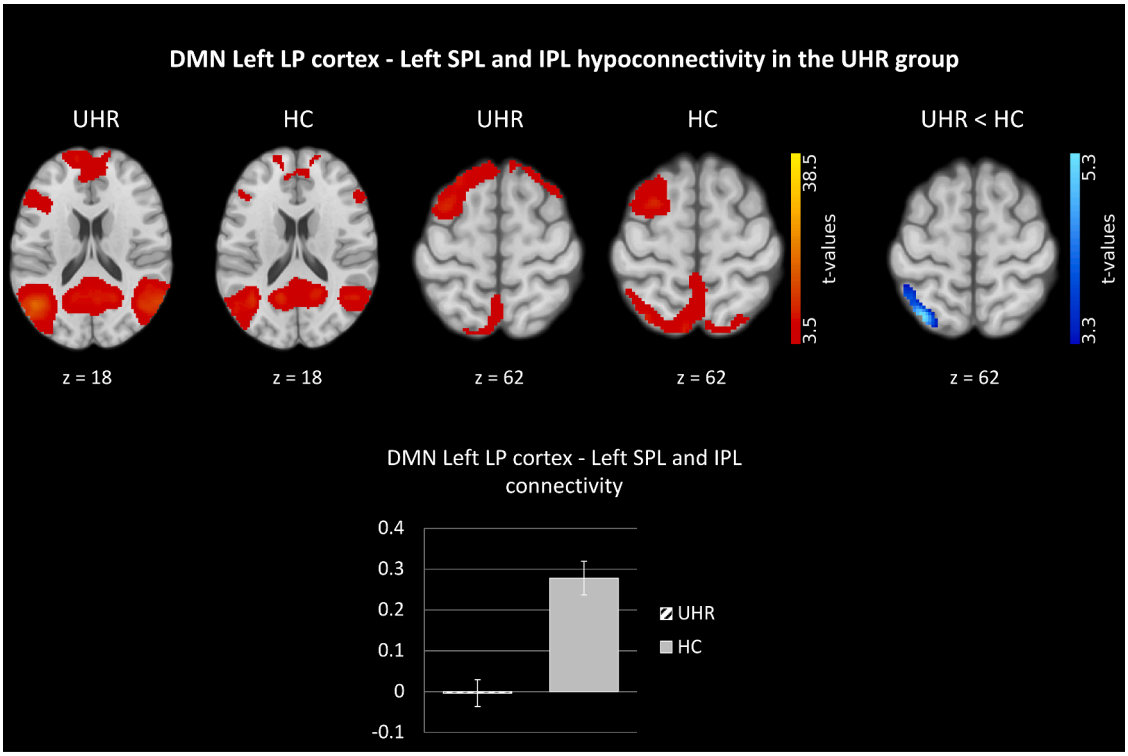


Fig. 4. Hypoconnectivity of the left lateral parietal (LP) cortex seed of the default mode network (DMN). The DMN connectivity maps using the left LP as seed region for both UHR and HC groups were shown. The UHR group ($N = 20$) displayed decreased functional connectivity with the left superior parietal lobule (SPL) and inferior parietal lobule (IPL) compared to HCs ($N = 16$) (cluster size: 388 voxels; $p_{FWE\text{-}corr} < 0.003$). The result is superimposed on the MNI-152-T1 standard image. Color map represents *t*-values. Bar graph indicates group-averaged z-values extracted from the significant cluster, while error bars represent standard errors.

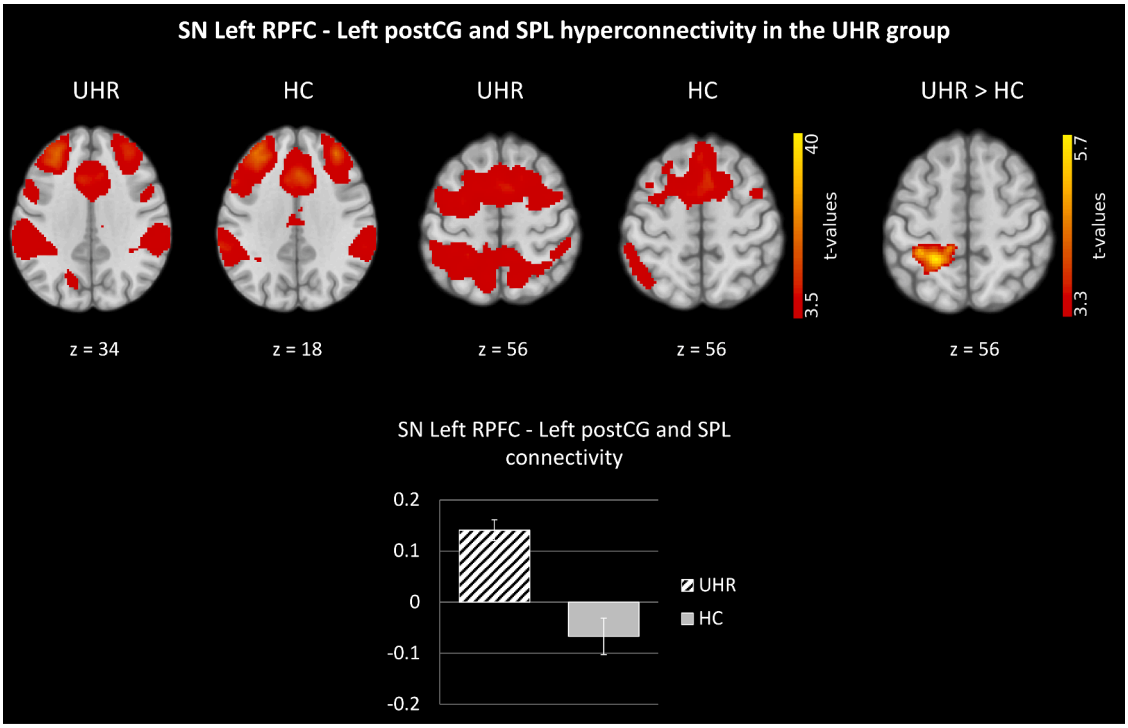


Fig. 5. Hyperconnectivity of the left rostral prefrontal cortex (RPFC) seed of the salience network (SN). The SN connectivity maps using the left RPFC as seed region for both UHR and HC groups were shown. The UHR group ($N = 20$) displayed increased functional connectivity with the left postcentral gyrus (postCG) and superior parietal lobule (SPL) compared to HCs ($N = 16$) (cluster size: 829 voxels; $p_{FWE\text{-}corr} < 0.001$). The result is superimposed on the MNI-152-T1 standard image. Color map represents *t*-values. Bar graph indicates group-averaged z-values extracted from the significant cluster, while error bars represent standard errors.

Perceptual deficits related with early visual processing and their contributions to cognitive impairments in schizophrenia are well documented (for a review see (Butler and Javitt, 2005)). More recent studies on gray matter volume loss (Zhao et al., 2018) and on aberrant rs-FC within the visual cortex (Li et al., 2018) of the UHR subjects are in support of our finding. While increase in the time-lagged correlations between a frontal network component that includes the MPFC node of the DMN and visual system components (Jafri et al., 2008) and an abnormal inter-network connectivity between the DMN and VN have been reported previously (Peng et al., 2021), an explicit report of clearly increased rs-FC of the DMN with the visual areas is a rather novel finding of the present study. Such facilitation of the signal transmission between these two networks or reduced modularity of the DMN in the form of an expansion towards the VN may point to one of the basic neuropathological processes in UHR that may lead to aberrant processing of the visual inputs related with visual hallucinations or delusions in later stages.

In the present study, we additionally found a decreased FC between the left LP cortex seed of DMN and the left DAN areas in UHR subjects. Since there was a concurrent increase of the SN connectivity to DAN, this result will be discussed below under SN results.

4.2. SN results

The SN, which includes two key nodes, the anterior insula (AI) and anterior cingulate cortex (ACC), is widely involved in cognitive and affective processing, with its crucial role in directing attention to relevant or salient stimuli (Seeley et al., 2007). Closely associated with the bottom-up salience attribution to external or internal events and the reward system, SN mediates a switch between the DMN and task-positive networks (TPN) (Conio et al., 2020; Menon, 2011). Many studies and meta-analyses on the psychosis spectrum have reported changes in both the intra- and inter-network rs-FCs of the SN (Brandl et al., 2019; Kraguljac et al., 2015; O'Neill et al., 2019; Wang et al., 2016; Wotruba et al., 2014), while results in opposing directions were reported in terms of decreased intrinsic connectivity of the SN in at-risk mental state vs increased intrinsic connectivity in unmedicated schizophrenia subjects (Kraguljac et al., 2015; Wang et al., 2016).

In the present study, the SN displayed increased rs-FC with right posterior node of SN itself, and bilateral SMN and DAN regions in UHR subjects. The increased intrinsic connectivity of the SN and its hyperconnectivity with the SMN may be associated with the aberrant salience attribution to external and internal events and reality distortions. A review on the opposite effects of the dopamine and serotonin on the resting-state networks (Conio et al., 2020) shows that the increased dopaminergic activity in the nigro-striatal system increases the intrinsic connectivity of the SMN, while the mesocortical dopamine increase leads to increased intrinsic connectivity in the SN, which nicely fits to our SN and SMN results in UHR. On the other hand, the more crucial result of the present study was the increased inter-network connectivity of the SN with DAN and SMN in the left hemisphere that was positively correlated with the Trail Making Test - B (TMT-B) score, which evaluates the working memory and set-shifting abilities (Arbuthnott and Frank 2000, Sánchez-Cubillo et al, 2009). Previous studies also reported impaired TMT-B performance in UHR subjects (Koutsouleris et al., 2009; Hubl et al., 2018), and associated this with co-existent abnormal metabolic activity of the dorsal striatum and disrupted cingulo-striatal FC in clinical high risk for psychosis subjects. The presence of a significant correlation between the TMT-B score and the SN to DAN and SMN connectivity values in the present study indicates a more direct and robust functional association between these processes. Vossel and colleagues (2014) suggested that the interplay between the ventral and dorsal attention networks is crucial for flexible and dynamic attentional control in relation to top-down and bottom-up processing. Hence, our finding of aberrant SN-DAN and SN-SMN internetwork hyperconnectivity positively correlated with the difficulties in TMT-B may restrain the flexible interactions between the two systems resulting in problems in visual search and visuomotor integration as well as set

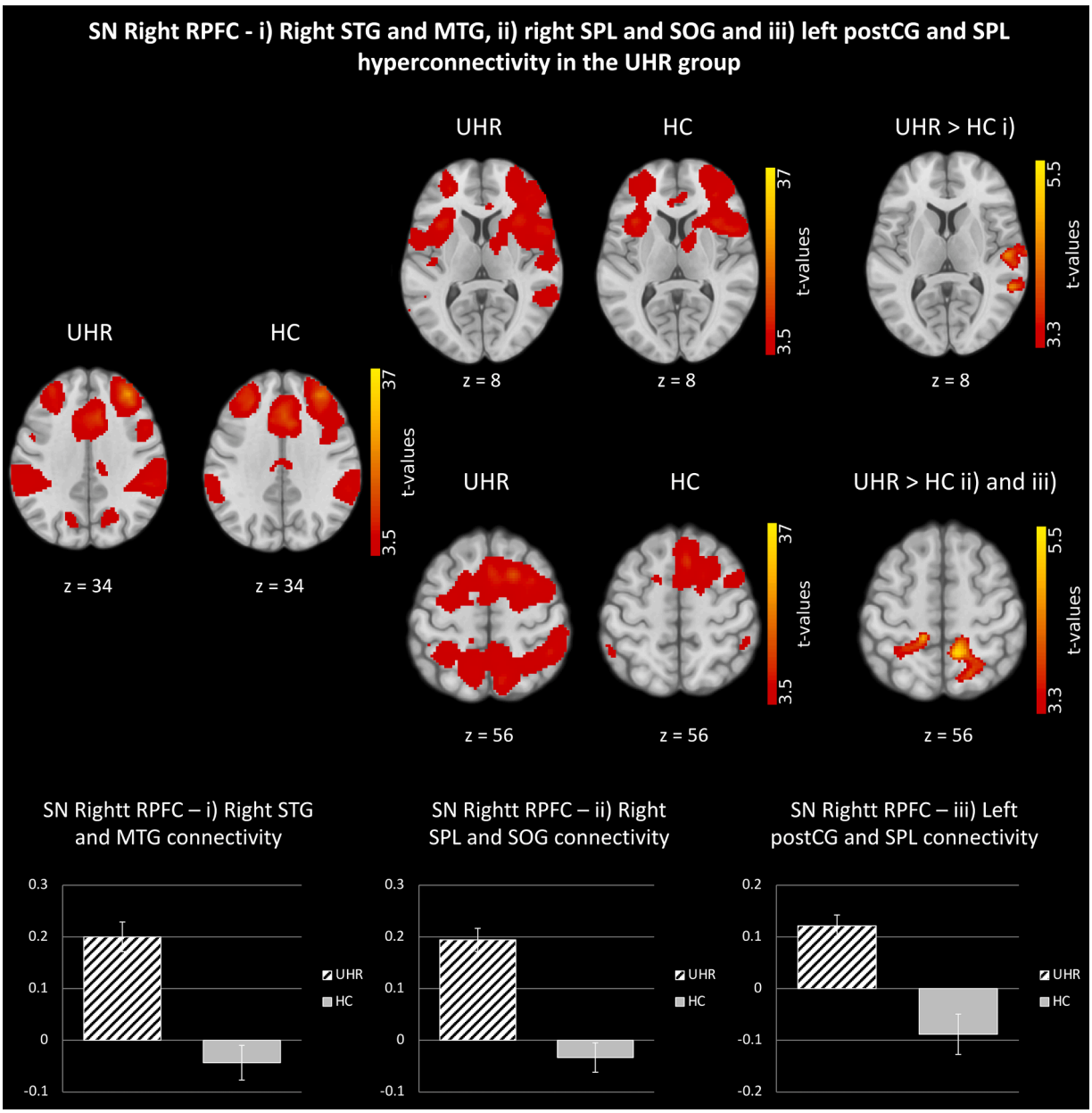


Fig. 6. Hyperconnectivity of the right rostral prefrontal cortex (RPFC) seed of the salience network (SN). The SN connectivity maps using the right RPFC as seed region for both UHR and HC groups were shown. The UHR group ($N = 20$) displayed increased functional connectivity (i) with the right superior temporal gyrus (STG) and middle temporal gyrus (MTG), (ii) with the right superior parietal lobule (SPL) and superior occipital gyrus (SOG), and (iii) with the left postCG and SPL compared to HCs ($N = 16$) (cluster size: 832 voxels, 749 voxels and 477 voxels, respectively, $p_{FWE\text{-}corr} < 0.001$). The result is superimposed on the MNI-152-T1 standard image. Color map represents *t*-values. Bar graphs indicate group-averaged z-values extracted from the 3 different significant clusters, while error bars represent standard errors.

shifting in UHR subjects.

4.4. Limitations

Our study has several limitations. Because of small sample size, we may lack enough power to detect associations. Secondly, we admitted participants from a tertiary center, which may limit the generalization of our results. Thirdly, we selected participants according to the CAARMS criteria, which focus more on positive symptoms. This might have excluded individuals at UHR with predominantly negative symptoms.

On the other hand, in order to protect from Type I errors, we applied Bonferroni correction for the number of seeds in rs-FC comparisons between the two groups, which is a strict and consequent solution to the multiple comparison problem. This may have increased the vulnerability to Type II error, resulting in false negative results related with the connectivity differences of the thalamus and amygdala seeds and the intra-network connectivity of the DMN, often reported in previous studies (Anticevic et al., 2015; Ho et al., 2019; O'Neill et al., 2019). However, as our aim was to identify the most robust FC features, the low sensitivity of the present statistics to relatively weaker differences does not create an important deficiency in the context of the present study.

4.3. Conclusion

In conclusion, our findings show that UHR individuals exhibit alterations in connectivity involving the SN and DMN relative to healthy controls, with a dominance of the SN findings, indicating the central role

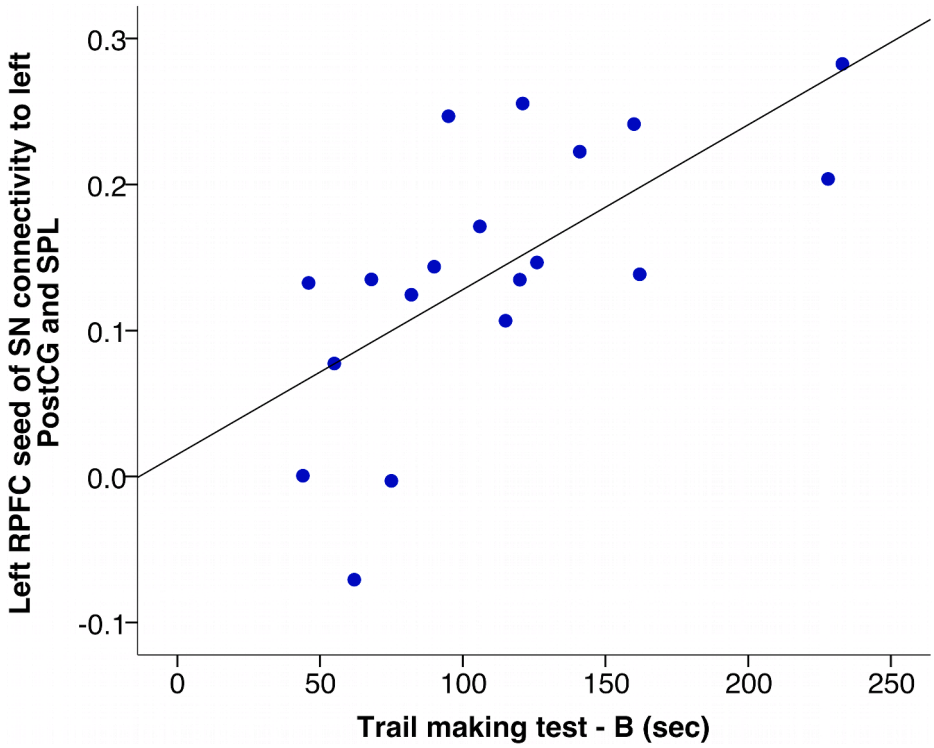


Fig. 7. Correlations between the mean functional connectivities and neuropsychological scores of UHR subjects. Left rostral prefrontal cortex (RPFC) seed of the salience network (SN) connectivity to the left postcentral gyrus (postCG) and superior parietal lobule (SPL) displayed positive correlation with TMT-B, indicating higher SN connectivity with posterior regions is associated with worse working memory and set-shifting performance on TMT-B ($r = 0.737$, $p = 0.0003$).

of this network and salience processing in UHR. Additionally, the SN connectivity to the left DAN and SMN, which significantly correlated with the behavioural cognitive measurements of the UHR subjects, is the crucial finding pointing to pathophysiological processes that already are in play in UHR, and hence may be important in the search for a biomarker of conversion to psychosis. In order to extend our results, our findings should be tested in longitudinal studies and with larger sample sizes.

Declaration of Competing Interest

The authors declare no conflict of interest related to this manuscript

Acknowledgement

This work was supported by the Scientific Research Projects Coordination Unit of Istanbul University (Project No. TTU- 2016-21613).

References

Addington, D., Addington, J., Maticka-Tyndale, E., Joyce, J., 1992. Reliability and validity of a depression rating scale for schizophrenics. Schizophr. Res. 6 (3), 201–208.

Allen, P., Chaddock, C.A., Egerton, A., Howes, O.D., Bonoldi, I., Zelaya, F., et al., 2016. Resting hyperperfusion of the hippocampus, midbrain, and basal ganglia in people at high risk for psychosis. Am. J. Psychiatry 173 (4), 392–399.

Andreasen, N., 1983. The Scale for the Assessment of Negative Symptoms (SANS). University of Iowa, Iowa City. IA.

Andreasen, N.C., 1984. Scale For the Assessment of Positive Symptoms (SAPS). University of Iowa.

Anteraper, S.A., Collin, G., Guell, X., Scheinert, T., Molokotos, E., Henriksen, M.T., et al., 2020. Altered resting-state functional connectivity in young children at familial high risk for psychotic illness: a preliminary study. Schizophr. Res. 216, 496–503. https://doi.org/10.1016/j.schres.2019.09.006.

Anticevic, A., Haut, K., Murray, J.D., Repovs, G., Yang, G.J., Diehl, C., et al., 2015. Association of thalamic dysconnectivity and conversion to psychosis in youth and young adults at elevated clinical risk. JAMA Psychiatry 72 (9), 882–891.

Arbuthnott, K., Frank, J., 2000. Trail making test, part B as a measure of executive control: validation using a set-switching paradigm. J. Clin. Exp. Neuropsychol. 22 (4), 518–528.

Bloomfield, P.S., Selvaraj, S., Veronese, M., Rizzo, G., Bertoldo, A., Owen, D.R., et al., 2016. Microglial activity in people at ultra high risk of psychosis and in schizophrenia: an [(11)C]PBR28 PET brain imaging study. Am. J. Psychiatry 173 (1), 44–52. https://doi.org/10.1176/appi.ajp.2015.14101358.

Borgwardt, S.J., Riecher-Rössler, A., Dazzan, P., Chitnis, X., Aston, J., Drewe, M., et al., 2007. Regional gray matter volume abnormalities in the at risk mental state. Biol. Psychiatry 61 (10), 1148–1156. https://doi.org/10.1016/j.biopsych.2006.08.009.

Brandl, F., Avram, M., Weise, B., Shang, J., Simões, B., Bertram, T., Hoffmann Ayala, D., Penzel, N., Gürsel, D.A., Bäuml, J., Wohlschläger, A.M., Vukadinovic, Z., Koutsouleris, N., Leucht, S., Sorg, C., 2019. Specific substantial dysconnectivity in schizophrenia: a transdiagnostic multimodal meta-analysis of resting-state functional and structural magnetic resonance imaging studies. Biol. Psychiatry 85 (7), 573–583. https://doi.org/10.1016/j.biopsych.2018.12.003.

Buckner, R.L., Andrews-Hanna, J.R., Schacter, D.L., 2008. The brain's default network: anatomy, function, and relevance to disease. Ann. NY Acad. Sci. 1124, 1–38. https://doi.org/10.1196/annals.1440.011.

Butler, PD, Javitt, DC, 2005. Early-stage visual processing deficits in schizophrenia. Current opinion in psychiatry 18 (2), 151–157. https://doi.org/10.1097/00001504-200503000-00008.

Chu, A.O.K., Chang, W.C., Chan, S.K.W., Lee, E.H.M., Hui, C.L.M., Chen, E.Y.H., 2018. Comparison of cognitive functions between first-episode schizophrenia patients, their unaffected siblings and individuals at clinical high-risk for psychosis. Psychol. Med. 18, 1–8.

Clark, S.V., Mittal, V.A., Bernard, J.A., Ahmadi, A., King, T.Z., Turner, J.A., 2018. Stronger default mode network connectivity is associated with poorer clinical insight in youth at ultra high-risk for psychotic disorders. Schizophr. Res. 193, 244–250. https://doi.org/10.1016/j.schres.2017.06.043.

Collin, G., Nieto-Castanon, A., Shenton, M.E., Pasternak, O., Kelly, S., Keshavan, M.S., et al., 2020. Brain functional connectivity data enhance prediction of clinical outcome in youth at risk for psychosis. NeuroImage. Clin. 26, 102108 https://doi.org/10.1016/j.nicl.2019.102108.

Conio, B., Martino, M., Magioncalda, P., Escelsior, A., Inglese, M., Amore, M., Northoff, G., 2020. Opposite effects of dopamine and serotonin on resting-state networks: review and implications for psychiatric disorders. Mol. Psychiatry 25 (1), 82–93.

Cooper, D., Barker, V., Radua, J., Fusar-Poli, P., Lawrie, S.M., 2014. Multimodal voxel-based meta-analysis of structural and functional magnetic resonance imaging studies in those at elevated genetic risk of developing schizophrenia. Psychiatry Res. 221 (1), 69–77.

Dandash, O., Fornito, A., Lee, J., Keefe, R.S., Chee, M.W., Adcock, R.A., et al., 2014. Altered striatal functional connectivity in subjects with an at-risk mental state for psychosis. Schizophr. Bull. 40 (4), 904–913.

Fusar-Poli, P., Deste, G., Smieskova, R., Barlati, S., Yung, A.R., Howes, O., et al., 2012a. Cognitive functioning in prodromal psychosis: a meta-analysis. Arch. Gen. Psychiatry 69 (6), 562–571.
Gifford, G., Crossley, N., Fusar-Poli, P., Schnack, H.G., Kahn, R.S., Koutsouleris, N., et al., 2017. Using neuroimaging to help predict the onset of psychosis. NeuroImage 145, 209–217.
Golden, J.C., 1978. Stroop Color and Word Test: A Manual for Clinical and Experimental Uses.. Chicago, IL: Stoelting Co.
Gong, J., Wang, J., Luo, X., Chen, G., Huang, H., Huang, R., Huang, L., Wang, Y., 2020. Abnormalities of intrinsic regional brain activity in first-episode and chronic schizophrenia: a meta-analysis of resting-state functional MRI. J. Psychiatry Neurosci. 45 (1), 55–68. https://doi.org/10.1503/jpn.180245.
Guo, W, Liu, F, Chen, J, Wu, R, Li, L, Zhang, S, Chen, H, Zhao, J, et al., 2017. Hyperactivity of the default-mode network in first-episode, drug-naive schizophrenia at rest revealed by family-based case-control and traditional case-control designs. Medicine 96 (13), e6223. https://doi.org/10.1097/MD.0000000000006223.
Heaton, R.K., Chelune, G.J., Talley, J.L., Kay, G.G., Curtiss, G., 1993. Wisconsin Card Sorting Test Manual Revised and Expanded. Psychological Assessment Resources Inc, Odessa, FL.
Ho, N.F., Li Hui Chong, P., Lee, D.R., Chew, Q.H., Chen, G., Sim, K., 2019. The amygdala in schizophrenia and bipolar disorder: a synthesis of structural MRI, diffusion tensor imaging, and resting-state functional connectivity findings. Harv. Rev. Psychiatry 27 (3), 150–164. https://doi.org/10.1097/HRP.0000000000000207.
Hou, C.L., Xiang, Y.T., Wang, Z.L., Everall, I., Tang, Y., Yang, C., et al., 2016. Cognitive functioning in individuals at ultra-high risk for psychosis, first-degree relatives of patients with psychosis and patients with first-episode schizophrenia. Schizophr. Res. 174 (1-3), 71–76.
Howes, O.D., Montgomery, A.J., Asselin, M.C., Murray, R.M., Valli, I., Tabraham, P., et al., 2009. Elevated striatal dopamine function linked to prodromal signs of schizophrenia. Arch. Gen. Psychiatry 66 (1), 13–20.
Hubl, D., Schultze-Lutter, F., Hauf, M., Dierks, T., Federspiel, A., Kaess, M., et al., 2018. Striatal cerebral blood flow, executive functioning, and fronto-striatal functional connectivity in clinical high risk for psychosis. Schizophr. Res. 201, 231–236.
Jafri, MJ, Pearlson, GD, Stevens, M, Calhoun, VD, et al., 2008. A method for functional network connectivity among spatially independent resting-state components in schizophrenia. Neuroimage.
Kim, H.S., Shin, N.Y., Jang, J.H., Kim, E., Shim, G., Park, H.Y., et al., 2011. Social cognition and neurocognition as predictors of conversion to psychosis in individuals at ultra-high risk. Schizophr. Res. 130 (1-3), 170–175.
Koutsouleris, N., Meisenzahl, E.M., Davatzikos, C., Bottlender, R., Frodl, T., Scheuerecker, J., et al., 2009. Use of neuroanatomical pattern classification to identify subjects in at-risk mental states of psychosis and predict disease transition. Arch. Gen. Psychiatry 66 (7), 700–712.
Kraguljac, NV, White, DM, Hadley, JA, Visscher, K, Knight, D, ver Hoef, L, Falola, B, Lahti, AC, et al., 2015. Abnormalities in large scale functional networks in unmedicated patients with schizophrenia and effects of risperidone. NeuroImage. Clinical.
Lee, W.H., Doucet, G.E., Leibu, E., Frangou, S., 2018. Resting-state network connectivity and metastability predict clinical symptoms in schizophrenia. Schizophr. Res. 201, 208–216.
Li, R.R., Lyu, H.L., Liu, F., Lian, N., Wu, R.R., Zhao, J.P., et al., 2018. Altered functional connectivity strength and its correlations with cognitive function in subjects with ultra-high risk for psychosis at rest. CNS Neurosci. Ther. 24 (12), 1140–1148.
Lukoff, D., Nuechterlein, K.H., Ventura, J., 1986. Manual for the expanded brief psychiatric rating scale. Schizophr. Bull. 12, 594–602.
Menon, V., 2011. Large-scale brain networks and psychopathology: a unifying triple network model. Trends Cogn. Sci. 15 (10), 483–506.
Morey, R.A., Inan, S., Mitchell, T.V., Perkins, D.O., Lieberman, J.A., Belger, A., 2005. Imaging frontostriatal function in ultra-high-risk, early, and chronic schizophrenia during executive processing. Arch. Gen. Psychiatry 62, 254–262.
O'Neill, A., Mechelli, A., Bhattacharyya, S., 2019. Dysconnectivity of large-scale functional networks in early psychosis: a meta-analysis. Schizophr. Bull. 45 (3), 579–590.
Pelletier-Baldelli, A., Andrews-Hanna, J.R., Mittal, V.A., 2018. Resting state connectivity dynamics in individuals at risk for psychosis. J. Abnorm. Psychol. 127 (3), 314–325.
Peng, Y., Zhang, S., Zhou, Y., Song, Y., Yang, G., Hao, K., Zhang, Y., 2021. Abnormal functional connectivity based on nodes of the default mode network in first-episode drug-naive early-onset schizophrenia. Psychiatry Res. 295, 113578.
Rey, A., 1964. L'Examen Clinique en Psychologie. Presses Universitaires de France, Paris.
Reitan, R.M., 1955. The relationship of the trail making test to organic brain damage. J. Consult. Psychol. 19, 39–393.
Sánchez-Cubillo, I., Periáñez, J.A., Adrover-Roig, D., Rodríguez-Sánchez, J.M., Ríos-Lago, M., Tirapu, J., Barceló, F., 2009. Construct validity of the trail making test: role of task-switching, working memory, inhibition/interference control, and visuomotor abilities. J. Int. Neuropsychol. Soc. JINS 15 (3), 438–450. https://doi.org/10.1017/S1355617709090626.
Schaefer, A., Kong, R., Gordon, E.M., Laumann, T.O., Zuo, X.N., Holmes, A.J., Yeo, B.T., 2018. Local-global parcellation of the human cerebral cortex from intrinsic functional connectivity MRI. Cereb. Cortex 28 (9), 3095–3114.
Seeley, W.W., Menon, V., Schatzberg, A.F., Keller, J., Glover, G.H., Kenna, H., et al., 2007. Dissociable intrinsic connectivity networks for salience processing and executive control. J. Neurosci. 27 (9), 2349–2356.
Sharma, A, Kumar, A, Singh, S, Bhatia, T, Beniwal, RP, Khushu, S, Prasad, KM, Deshpande, SN, et al., 2018. Altered resting state functional connectivity in early course schizophrenia. Psychiatry research. Neuroimaging, 271, 17–23. https://doi.org/10.1016/j.pscychresns.2017.11.013. Neuroimaging.
Shim, G., Oh, J.S., Jung, W.H., Jang, J.H., Choi, C.H., Kim, E., et al., 2010. Altered resting-state connectivity in subjects at ultra-high risk for psychosis: an fMRI study. Behav. Brain Funct. 6, 58. https://doi.org/10.1186/1744-9081-6-58.
Üçok, A., Direk, N., Koyuncu, A., Keskin-Ergen, Y., Yüksel, Ç., Güler, J., et al., 2013. Cognitive deficits in clinical and familial high risk groups for psychosis are common as in first episode schizophrenia. Schizophr. Res. 151 (1-3), 265–269.
Vossel, S., Geng, J.J., Fink, G.R, 2014. Dorsal and ventral attention systems: distinct neural circuits but collaborative roles. Neuroscientist 20 (2), 150–159. https://doi.org/10.1177/1073858413494269 a review journal bringing neurobiology, Neurology and psychiatry.
Wang, C., Ji, F., Hong, Z., Poh, J.S., Krishnan, R., Lee, J., et al., 2016. Disrupted salience network functional connectivity and white-matter microstructure in persons at risk for psychosis: findings from the LYRIKS study. Psychol. Med. 46 (13), 2771–2783. https://doi.org/10.1017/S0033291716001410.
Wechsler, D, 1981. Manual for the Wechsler adult intelligence scale-revised. New York: Psychological Corporation.
Whitfield-Gabrieli, S., Nieto-Castanon, A., 2012. Conn: a functional connectivity toolbox for correlated and anticorrelated brain networks. Brain Connect. 2 (3), 125–141.
Wotruba, D., Michels, L., Buechler, R., Metzler, S., Theodoridou, A., Gerstenberg, M., et al., 2014. Aberrant coupling within and across the default mode, task-positive, and salience network in subjects at risk for psychosis. Schizophr. Bull. 40 (5), 1095–1104.
Yokuşoğlu, Ç., Ercis, M., Çağlar, N., Aydemir, Ö., Üçok, A., 2020. Reliability and validity of the Turkish version of comprehensive assessment of at risk mental states. Early Interv. Psychiatry. https://doi.org/10.1111/eip.13014. Advance online publication. 10.1111/eip.13014.
Yung, A.R., Yuen, H.P., McGorry, P.D., Phillips, L.J., Kelly, D., Dell'Olio, M., et al., 2005. Mapping the onset of psychosis: the comprehensive assessment of at-risk mental states. Aust. N. Z. J. Psychiatry 39 (11-12), 964–971.
Zhao, C., Zhu, J., Liu, X., Pu, C., Lai, Y., Chen, L., et al., 2018. Structural and functional brain abnormalities in schizophrenia: A cross-sectional study at different stages of the disease. Prog. Neuropsychopharmacol. Biol. Psychiatry 83, 27–32. https://doi.org/10.1016/j.pnpbp.2017.12.017.
Zhu, F., Liu, Y., Liu, F., Yang, R., Li, H., Chen, J., et al., 2019. Functional asymmetry of thalamocortical networks in subjects at ultra-high risk for psychosis and first-episode schizophrenia. Eur. Neuropsychopharmacol. 29 (4), 519–528.